Discovery of Functional Luminescence Properties Based on Flexible and Bendable Boron-Fused Azomethine/Azobenzene Complexes with O,N,O-Type Tridentate Ligands

Masayuki Gon, Kazuo Tanaka* and Yoshiki Chujo

Department of Polymer Chemistry, Graduate School of Engineering, Kyoto University

Katsura, Nishikyo-ku, Kyoto 615-8510, Japan

E-mail: tanaka@poly.synchem.kyoto-u.ac.jp

graphical Table of Contents
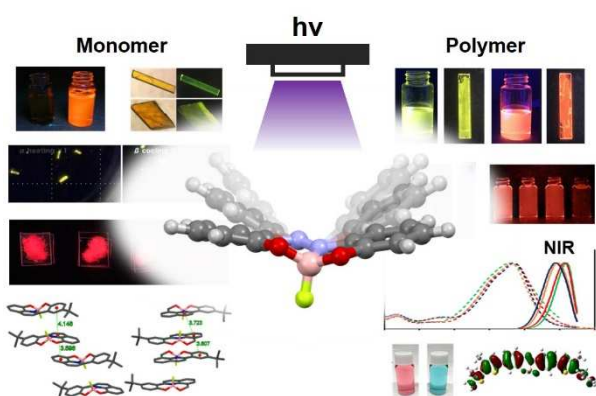
Flexible and bendable complexes: The boron-fused azomethine and azobenzene complexes with the O,N,O-type tridentate ligands showed unique optical properties including AIE and CIE. The π-conjugated polymers exhibited highly efficient emission from yellow to NIR region both in solution and film states.

Masayuki Gon

Masayuki Gon earned his Ph.D. in Polymer Chemistry from Kyoto University in 2016. He developed three-dimensionally-arranged π-conjugated materials and studied their specific optical and physical properties based on structure and chirality. He worked as a visiting research fellow in the group of Prof. Kenneth J. Wynne at Virginia Commonwealth University in America, in 2014. Now, he is an assistant professor of Department of Polymer Chemistry, Graduate School of Engineering, Kyoto University since 2016. His present research theme is development of functional π-conjugated materials focused on unique nature of heteroatoms.

Kazuo Tanaka

Kazuo Tanaka received his Ph.D. degree in 2004 from Kyoto University, and worked in Stanford University, USA, Kyoto University, and RIKEN as a postdoctoral fellow. In 2007, he has moved to the Department of Polymer Chemistry, Graduate School of Engineering, Kyoto University, and in 2018, he was promoted to Professor. His research projects especially focus on design of new functional materials relating optics and nanotechnology based on the heteroatom-containing conjugated polymers and organic-inorganic polymer hybrids.

Yoshiki Chujo

Yoshiki Chujo completed his Ph.D. at Kyoto University in 1980. After working at Nagoya University, Virginia Tech in USA, and Kyoto University, he has been Professor at Kyoto University during 1994-2018. He is now a Professor Emeritus of Kyoto University, Director of Digital Monozukuri Education &

Research Center of Hiroshima University, and Professor of Ritsumeikan University, Doshisha University, and National Taiwan University. His research interests focus on polymer synthesis and organic-inorganic hybrid materials.

Abstract

Azomethine (C=N) and azo (N=N) scaffolds are a part of structural units in poly(*p*-phenylene azomethine) (PAM) and poly(*p*-phenylene azo) (PAZ), respectively. Poly(*p*-phenylene vinylene) (PPV) is known to be one of luminescent π-conjugated polymers, meanwhile PAM and PAZ, which is the aza-substituted PPV analogues, are regarded as weak or no emissive materials. However, by the boron complexation, intense emission can be induced. Furthermore, environment-sensitivity and stimuli-responsivity were also observed. In this review, we demonstrate unique and versatile luminescent properties based on "flexible and bendable" π-conjugated systems composed of the boron-fused azomethine and azobenzene complexes (BAm and BAz) with the O,N,O-type tridentate ligands. The "flexible and bendable" luminophores showed intriguing optical behaviors, such as thermosalient effect, aggregation-induced emission (AIE) and crystallized-induced emission (CIE). Moreover, highly efficient emissions both in solution and film states were observed from the polymers. We illustrate the results and mechanisms on these luminescent properties from the series of our recent studies with BAm and BAz complexes and polymers.

Introduction

Various types of luminescent materials have been developed and now play essential roles in commodity devices used in our daily lives. From the discovery of the blue-emissive inorganic material, light sources in the optical devices, such as illuminations, traffic lights and displays, have been replaced to light-emitting devices (LEDs).[1,2] More recently, organic light emitting diodes (OLEDs) gradually become popular as an alternative light source because of the advantages, such as lightness, wide visible angle and low power consumption.[3,4] Furthermore, organic materials have been expected to be a key component for developing wearable devices.[5] For realizing these advanced devices, π-conjugated polymers have attracted much attention as a platform because of intrinsic advantages, such as high conductivity, film-formability, processability and flexibility.[6,7] Indeed, a lot of polymer-based organic photovoltaics (OPVs)[8] and OLEDs[9] have been already developed.

Poly(*p*-phenylene vinylene) (PPV) is one of conventional π-conjugated polymers and widely used both in industry and research fields.[10] From the first report on π-conjugated polymer-based OLEDs with PPV,[11] so far various-types of organic optoelectronic devices have been fabricated.[12] As mentioned here, PPV is very famous as a luminescent material, while poly(*p*-phenylene azomethine) (PAM) and poly(*p*-phenylene azo) (PAZ), where one or two vinylene carbon atoms are replaced into nitrogen atoms, respectively, are known to be weak or non-emissive frameworks (Figure 1a).[13,14] It is proposed that electronic coupling between lone pairs of nitrogen and π-conjugation should inhibit electronic interaction through main chains.[13] In addition, *N*-benzylideneaniline (azomethine) and azobenzene, which are the monomeric units of PAM and PAZ, respectively, have photoreactivity.[15,16] Thus, PAM and PAZ have been

hardly used as a scaffold for luminescent materials. So far, the PAM scaffold is often utilized for constructing covalent organic frameworks (COFs).[17] The PAZ scaffold has been applied as a photo-switchable unit based on *cis–trans* photoisomerization of azobenzene[18] and as a rigid mesogenic skeletons for liquid crystals.[19]

From theoretical calculations, lower energy levels of HOMO (highest occupied molecular orbital) and LUMO (lowest unoccupied molecular orbital) are obtained from PAM and PAZ than those of PPV (Figure 1b).[20] Although degree of perturbation effects by replacing carbon to nitrogen on the energy levels of HOMO and LUMO is different, the conjugated systems are mostly stabilized by the substitution to electron-negative nitrogen. Since HOMO and LUMO energy levels and energy gaps directly influence on physical properties of materials, such as carrier transport ability, light-absorption ability and emission color, the nitrogen substitution by the replacement of the vinyl unit to PAM or PAZ is a valid strategy not only for improving device efficiency but also for development of optoelectronic materials.

Recently, we have proposed the design concept based on "element-blocks" which is a minimum functional unit containing heteroatoms.[21–23] Originating from unique properties of heteroatoms, a wide variety of luminescent dyes and polymers have been developed based on this concept. We have focused on boron to induce luminescent properties from the series of non-emissive ligands including PAM and PAZ structures. In general, the boron complexation is effective for inducing luminescent properties by improving molecular rigidity and planarity.[24,25] This effect can work in PAM and PAZ. In particular, although *cis–trans* photoisomerization are inevitable in the free PAM and PAZ, these energy-consumable conformational changes can be efficiently suppressed by the boron complexation. Furthermore, electronic transition from non-bonding orbitals

including the nitrogen lone pair to π* orbitals attributable to the forbidden transition is transformed to be the allowed one by the boron complexation.[26] As a result, intense emission can be observed from boron complexes. Indeed, several examples of luminescence from the azomethine and azobenzene derivatives have been reported.[26–38]

Commodity boron complexes are constructed with a series of bidentate ligands,[24,25] whereas we newly focus on the tridentate structures. Initially, we explain the unusual behaviors of the boron complexes with the azomethine and azobenzene tridentate ligands. By employing the O,N,O-type tridentate ligands, such as *o*-salicylideneaminophenol and 2,2′-dihydroxyazobenzene, the ring-fused structures are obtained, respectively (Figure 2). The syntheses of these complexes have been already accomplished in 1970–1980s,[39–41] while their luminescence properties are still veiled.[42–44] To clarify the optical properties, we designed and synthesized the boron-fused azomethine and azobenzene complexes (BAm and BAz). Interestingly, significant emissions were hardly detected from the solution samples containing these complexes.[45,46] These are unusual in comparison to the other bidentate boron complexes with the azomethine and azobenzene moieties as well as commodity molecules.[26–38] Surprisingly, enhanced emissions were obtained in the aggregation state. This phenomenon is called aggregation-induced emission (AIE) or aggregation-induced emission enhancement (AIEE).[47,48] Conventional organic luminophores show aggregation-caused quenching (ACQ) caused by non-specific intermolecular interactions in the condensed state,[49] meanwhile AIE-active molecules can show opposite behaviors such as solution annihilation and solid-state emission. Although various examples to offer such enhanced emission by solidification have been

recently reported, the AIE properties of the azomethine and azobenzene boron complexes should have unique mechanisms.

In comparison to the previous AIE molecules, the most impressive point is the structural features of the complex skeletons. Commodity AIE-active molecules usually have rotational and/or vibrational substituents which cause deactivation of excited energy through non-radiative processes in solution.[47] On the other hand, the azomethine and azobenzene complexes show AIE behaviors in the absence of movable substituents. We assumed from theoretical calculations that the extraordinary emission quenching of BAm and BAz units should be caused by intramolecular motions of the "flexible and bendable" structures (Figure 3).[45,46,50] In the excited state, since the bond lengths of C=N and N=N are elongated by about 0.1 Å from the ground state, the tightly ring-fused molecules could bend to release structural distortion. Consequently, intramolecular motions should be generated, resulting in emission annihilation in solution. In contrast, these molecular motions would be suppressed in solid, and excitation states can be maintained. Further, it is supposed that the protruded substituent at the boron atom should contribute to avoiding ACQ. Finally, the azomethine and azobenzene boron complexes can show crystallized-induced emission (CIE)[51] as well as AIE.

We also reported a series of AIE and CIE properties of boron ketoiminate[52–56] and boron diiminate[57–62] complexes using O,N or N,N-type bidentate ligands, respectively. From emission enhancement under frozen conditions, the "flexibility" in the excited state is a key factor for presenting AIE and CIE. Including these results, we recently proposed a new concept, "excitation-driven boron complexes" which show larger degree of structural relaxation in the excited state.[50] By restricting these motions,

stimuli-responsive optical properties including AIE and CIE are produced. The azomethine and azobenzene boron complexes are also classified in excitation-driven molecules.

By the introduction of these complexes into the polymer main chains, other characters can be induced. Highly-efficient emission in the near-infrared (NIR) region is observed both in solution and film states from donor–acceptor (D–A) type π-conjugated copolymers. This is because of intrinsic strong electron-accepting ability of the complexes. Low-lying LUMO energy levels of the PAM and PAZ scaffolds are additionally lowered by the B–N coordination, followed by extremely-narrow energy gaps between frontier molecular orbitals (FMOs).[63] Considering that the PPV scaffold usually works as a donor moiety,[64] the opposite electron-accepting properties of the PAM and PAZ scaffold are of interest and useful for constructing functional π-conjugated polymers. Furthermore, we found that construction of the PPV-like structure with alternating copolymerization between BAz and vinylene units achieved NIR absorption and emission although there were no electron-donating units.[65] Although the wavelengths of absorption and emission of PPV are limitedly from blue to orange region,[66,67] narrow energy gap between FMOs in ground and excited states can be achieved by employing the PAM and PAZ structures. We also mention the mechanisms later.

In this review, we initially introduce that "flexible and bendable" structures of boron complexes with the O,N,O-type tridentate ligands composed of the PAM and PAZ moieties are the origin of a lot of unprecedented optical properties, such as AIE, CIE and stimuli-responsive luminochromic behaviors. Next, we explain optical properties of the PAM and PAZ-containing polymers. We found that the Migita–Kosugi–Stille cross

coupling reaction[68,69] was a reliable manner for preparing main chain-type polymers without decomposition of the BAm and BAz complexes. As a result, the series of polymers can be obtained, and their optical properties originating from their electronic structures have been revealed. Recent results including the first discovery of unique functionalities of the BAm and BAz complexes and their mechanism are illustrated here.

1. Boron-fused azobenzene (BAz) complexes

Azobenzene, the partial structural unit in PAZ, is well known as a conventional dye and can be prepared by diazocoupling or oxidation from aniline derivatives.[70] A lot of unique properties including *cis–trans* photoisomerization, absorption in long-wavelength region and a rigid rod-like structure have been found and applied for photo-switchable materials,[71] dyes[72] and a mesogenic group of liquid crystals,[73] respectively. In addition, azobenzene is also well-known to a non-emissive scaffold due to fast internal conversion and excited deactivation through the non-radiative deactivation processes accompanied to the photoisomerization.[74–77] Although many challenges to obtain luminescence from azobenzene derivatives have been carried out on the basis of the strategies for suppressing photoisomerization, such as constructing metal complexes,[78] hydrogen bonding,[79–81] highly crystalline structures,[82,83] cyclic compounds[84], it is still difficult to observe intense emission from the azobenzene scaffold. Kawashima and coworkers successfully obtained significant emission from the azobenzene scaffold by the boron complexation at the N=N bond.[26] The resulting B–N coordination plays two critical roles in expressing emission. Firstly, the photoisomerization is efficiently suppressed. Since non-radiative deactivation is prohibited, excitation energy can be preserved. Next, the electronic state is drastically rearranged to that in favor of emission. The HOMO–LUMO transition is transformed from the forbidden n–π* character to the allowed π–π* one by the formation of the B–N coordination.[26] Thus, intense emission can be observed. As the next strategy for creating luminescent azobenzene derivatives, we proposed tightly-fused structures with O,N,O-type tridentate ligands, BAz. By using BAz complexes, we obtained AIE and CIE-active compounds as well as NIR-emissive π-conjugated polymers. In this section,

we introduce the details from the first discovery to recent results about the BAz complexes.

1.1 Discovery of AIE and NIR emission

The standard structure of BAz was synthesized by the reaction between commercially-available 2,2′-dihydroxyazobenzene (**LAz**) and boron trifluoride ethyl ether complex (BF$_3$·Et$_2$O) in triethylamine (Et$_3$N) and toluene at 100 °C (Figure 4a).[46] The yellow color of 2,2′-dihydroxyazobenzene turned to red, and the BAz complex (**BAz-H**) was obtained. The single crystal structure of **BAz-H** clearly showed tightly ring-fused structure and the perpendicularly-protruding fluorine atom from azobenzene scaffold (Figure 4b). The asymmetric structure provided a stereogenic boron center and the crystal packing showed that **BAz-H** obtained as a racemic crystal composed of *S* and *R* isomers. These enantiomers were able to be successfully separated by a chiral high performance liquid chromatography (HPLC). The circular dichroism (CD) of enantiomers showed the mirror-image Cotton effect. **BAz-H** showed a strong absorption band in long-wavelength region (λ_{abs} = 479 nm), meanwhile **Az-H**, a pristine azobenzene model compound, exhibited a typical azobenzene behavior, a strong absorption band in shorter wavelength region (λ_{abs} = 350~400 nm) and a weak absorption band in longer wavelength region (λ_{abs} = 400~500 nm) (Figure 4c). The effect of boron coordination is well explained by theoretical calculations with density functional theory (DFT) and time-dependent (TD) DFT. The non-bonding HOMO of azobenzene is stabilized by boron coordination, and the π-bonding molecular orbital becomes HOMO in **BAz-H** (Figure 4d). As a result, the forbidden S$_0$→S$_1$ (n–π*) transition of azobenzene is transformed to the allowed S$_0$→S$_1$ (π–π*) one.

Despite of the allowed $S_0 \rightarrow S_1$ (π–π*) transition of **BAz-H**, the complex showed faint emission (Φ_{PL} < 0.001, Φ_{PL}: absolute photoluminescence quantum efficiency) in the diluted solution (1.0×10^{-5} M in chloroform and 1.0×10^{-4} M in 1,4-dioxane) (Figure 4e). This behavior was different from the other boron complexes already reported.[26–38] In contrast, the emission is enhanced in the aggregation state (Φ_{PL} = 0.023, 1.0×10^{-4} M in 1,4-dioxane/H_2O = 1/99 v/v). The emission enhancement was also observed in a polymer matrix (Φ_{PL} = 0.007, 1 wt% **BAz-H** included polymethyl methacrylate (PMMA)). Those results indicate that **BAz-H** is an AIE-active molecule, and degree of intramolecular motions is responsible for emission enhancement. As mentioned above, commodity AIE-active dyes have multiple benzenes, while **BAz-H** can show AIE in the absence of exocyclic substituents. Thus, the AIE from tightly fused structures should be very rare.[85] We were able to obtain clues from estimation of the optimized molecular geometries both in the ground and excited states by TD-DFT calculations (Figure 5). Comparing to the C–N=N–C dihedral angle (φ) of the slightly bent azobenzene moiety (φ = 165°), the obviously bent structure in the excited state (φ = 141°) was obtained. The nitrogen–nitrogen double bond (N=N) was elongated by 0.10 Å from the ground state (1.27 Å) to the excited state (1.37 Å). The tightly ring-fused structure was critically affected by structural alteration, and the elongation should result in structural bent in the excited state. Therefore, in aggregation, such a molecular motion in the excited state is restricted, followed by emission enhancement.

Interestingly, π-conjugated copolymers with the BAz and bithiophene units (**P-BAz**) showed highly-efficient NIR emission even in the solution state (Figure 6) owing to strong D–A interaction with high electron-accepting ability of the BAz unit (LUMO energy level: −3.98 eV), whereas the non-fused azobenzene polymer (**P-Az**)

hardly exhibited emission. The **P-BAz** exhibited distinct solvatochromism of emission bands. The bathochromic shifts of the luminescence spectra were observed in polar solvents and the Lippert−Mataga plots revealed that the emission should be from the charge transfer (CT) state originating from the strong D–A interaction. From the oligomer models of mono-thiophene (**BAz-M1**) and bithiophene (**BAz-M2**), it was clearly proved that emission in solution was caused by extension of π-conjugation. As increasing π-conjugated units, both gradual increase in a radiative constant (k_r) and decrease in a non-radiative constant (k_{nr}) were detected. The restriction of the molecular motion and delocalization of π-electron through the polymer main chain should be responsible for these kinetics changes. The first study of BAz complexes strongly suggested that tightly-fused but slightly bent π-conjugated structure was a key factor for creating novel functional materials, for example, stimuli-responsive materials with AIE and NIR emission. These data suggest that the BAz complexes are a promising "element-block" for obtaining functional luminescent materials.

1.2. Tuning MO energy levels with substitution at 5,5′ positions

We observed highly efficient NIR emission from the polymers with the connection at 4,4′ positions in the BAz complex. By focusing on HOMO and LUMO distributions in **BAz-H**, a unique character is clarified. At the 5,5′-positions, large orbital coefficients in HOMO are obtained, while there are the nodes in LUMO (Figure 7a).[86] From these specially-separated FMOs, intriguing substitution effects can be expected. At first, we compared the substituent effects by bromination on optical properties. Accordingly, the narrower energy gap between FMOs was observed from 5,5′-substituted BAz (**BAz-5Br**) than that of 4,4′-substituted one (**BAz-4Br**) (Figure 7b). Interestingly, UV–

vis absorption and cyclic voltammetry (CV) suggested that the bromination at the 5,5′ positions induced the elevation of HOMO and the reduction of LUMO energy levels. DFT calculation disclosed that this anisotropic perturbation should be originated from the resonance and inductive effects on the energy levels of HOMO and LUMO depending on the degree of electron distribution of MOs, respectively. At the 5,5′ positions, because of large orbital coefficients of HOMO, the energy level is mainly affected by the resonance effect, while only the inductive effect can perturb energy levels of LUMO through the inductive effect because of very small orbital coefficients at these positions.

On the basis of the unique substituent effect, drastic reduction of LUMO energy levels was achieved by the modification at the 5,5′ positions. The π-conjugated copolymer BAz and bithiophene units connected at the 5,5′ positions (**P-BAz-5BT**) had a low LUMO energy level than the copolymer at the 4,4′ positions (**P-BAz-4BT**) (Figure 8a). Corresponded to the low LUMO energy level, large bathochromic shift of the emission band was observed, whereas Φ_{PL} was hardly enhanced. From the analyses of HOMOs and LUMOs of the model compounds (**M-BAz-5BT-Me** and **M-BAz-4BT-Me**), orthogonal perturbation depending on the substituent positions was also detected. Extension of HOMO and localization of LUMO are obtained when connected at the 5,5′ positions, and extension of both HOMO and LUMO at the 4,4′ positions (Figure 8b). In summary, by selecting the substituent positions, different effects on energy levels of FMOs, followed by optical properties can be obtained. Substitutions at the 4,4′ positions dramatically enhanced luminescence properties, and those at the 5,5′ positions effectively tuning MO energy levels. The controllable optical

properties of the BAz moiety are useful for designing optoelectronic properties to realize NIR-emissive and carrier-transport materials.

1.3. Enhancement of solid-state emission with substitution at boron

Next, we focused on the substituent effect on the perpendicularly-protruded substituent at the boron atom.[87] Most of organic luminophores usually show poor emission in the solid state due to ACQ caused by non-specific intermolecular interaction, such as π–π stacking.[49] In particular, development of solid-state NIR emissive materials has been still challenging because the NIR-emissive scaffolds tend to have extended π-conjugated systems which readily form π–π stacking.[88] As a consequence, critical ACQ is often induced. Because of wide versatility of NIR light especially for recognition and bioimaging, highly-efficient luminophores are still required.[88–90] To meet these demands, new design strategy for NIR-emissive materials is of significance. Herein, we explain the strategy for obtaining solid-state NIR-emissive polymers having perpendicularly-protruded aryl substituents at boron to preserve π-conjugated main chain from intermolecular interaction.

We synthesized a series of the BAz complexes, **BAz-C6F5**, **BAz-Ph** and **BAz-Mes**, with the perpendicularly-protruded aryl derivatives at the boron atom toward π-conjugated systems (Figure 9a). As a model polymer, we also prepared **BAz-F** with the perpendicularly-protruded fluorine substituent. From the optical measurements, the order of the wavelengths of absorption maxima of the BAz complexes seemed to be correlated with the type of the substituent at boron. By increasing electron-donating ability, the bathochromic effects on the absorption bands were observed. This means that the perpendicularly-protruded substituents at the boron atom are able to perturb the

electronic properties of the BAz complexes in the ground states. From the luminescent measurements, it was clearly demonstrated that these complexes had CIE properties. The emission intensity was obviously small in solution ($\Phi_{PL} < 0.01$) as detected in the series of BAz complexes, whereas intense emission was obtained in crystal (Figure 9a). It is likely that the perpendicularly-protruded substituents should play significant roles in inhibition of intermolecular interaction in condensed state, followed by CIE.

The substituents at the boron atom efficiently suppress intermolecular interaction even in π-conjugated polymers. To evaluate luminescent properties of the polymers in film, we synthesized alternating copolymers with BAz and bithiophene units, **P-BAz-F**, **P-BAz-C6F5**, **P-BAz-Ph** and **P-BAz-Mes** (Figure 9b). The polymers show good NIR luminescence in solution (λ_{PL} = 736~767 nm, Φ_{PL} = 0.04~0.15 for aryl substituents, λ_{PL} = 751 nm, Φ_{PL} = 0.25 for fluorine). As described in the other sections, substituent at 4,4′ positions enhanced emission properties. Furthermore, the emission properties are almost preserved even in film (λ_{PL} = 787~816 nm, Φ_{PL} = 0.05~0.09 for aryl substituents, λ_{PL} = 818 nm, Φ_{PL} = 0.04 for fluorine). LUMO energy levels were lowered by introducing the electron-accepting group (−3.94 eV for **P-BAz-F** and −3.92 eV for **P-BAz-C6F5**) and elevated by the electron-donating groups (−3.79 eV for **P-BAz-Ph** and −3.82 eV for **P-BAz-Mes**), meaning that color tuning is applicable by the substituent effect at the boron atom. From mechanistic studies including theoretical calculations, it was shown that electronic interaction was allowable between the aryl substituent to the π-conjugated system through the tetracoordinated boron (Figure 9a). It should be emphasized that the molecular weights of the monomeric unit in the polymer are relatively-low comparing to the previous NIR-emissive materials. The aza-substitution is reasonable for realizing solid-state emission in the NIR region.

1.4. NIR absorptive and emissive π-conjugated polymers

In previous sections, we mainly discussed electronic properties of D–A type π-conjugated polymers with the BAz units. By applying strong electron-accepting ability of the BAz unit (LUMO energy level: −3.8~4.0 eV), we obtained the highly-efficient NIR emissive polymers with strong D–A interactions. It should be noted that the BAz unit itself has a narrow energy gap between FMOs. In this section, we introduce the non D–A type π-conjugated polymer consisting of the alternating structure with the BAz and vinylene units (**BAz-PPV**).[65]

BAz-PPV was synthesized by Migita–Kosugi–Stille cross coupling reaction[68,69] with *trans*-1,2-bis(tributylstannyl)ethylene and the BAz comonomer (Figure 10a). Long branched alkyl chains were required for improving solubility in common organic solvents, such as toluene, chloroform and dichloromethane. As a reference polymer, pristine azobenzene containing one (**Az-PPV**) was also prepared. Surprisingly, **BAz-PPV** showed NIR absorption and emission in toluene (λ_{abs} = 702 nm, λ_{PL} = 760 nm and Φ_{PL} = 0.02), whereas **Az-PPV** showed shorter absorption maximum wavelength (λ_{abs} = 510 nm) and no emission under the same solution condition (Figure 10b). The difference in the peak wavelengths of the absorption bands should be caused by the intrinsic energy gap of π–π* transition in the monomers (**BAz**: $\lambda_{abs,edge}$ = 574 nm, 2.16 eV, **Az**: $\lambda_{abs,edge}$ = 451 nm, 2.75 eV). The elevation of HOMO and the reduction of LUMO energy levels were detected from the comparison with the monomers and polymers, meaning that π-conjugation should be extended through polymer main chains (Figure 10c). It should be mentioned that the length of π-conjugation was estimated to

be over 50 monomer units in the ground state from investigation of molecular weight-dependent absorption spectra.

Moreover, the polymer shows high stability toward photo-degradation and sufficient carrier-transport ability which is essential for the applications to organic semiconducting devices. From time-of-flight (TOF) technique,[91] the carrier mobility of **BAz-PPV** was calculated to be $10^{-2} \sim 10^{-3}$ cm^2 V^{-1} s^{-1}, and both hole and electron flew to the same degree (Figure 10d). In addition, carrier mobility of **Az-PPV** was similar. The values were higher than those of the reported PPV derivatives[92–94] and the other conventional π-conjugated polymers.[95–98] Therefore, it is proposed that introduction of the N=N double bonds might be effective for enhancing career mobility of π-conjugated polymers. It is presumable that the protruding fluorine atom by boron complexation might reduce the carrier transport ability due to inhibition of consecutive intermolecular π–π interactions. However, our data suggest that the carrier transport pathway in the bulk system should not be disturbed by introducing boron atoms.

2. Boron-fused azomethine (BAm) complexes

Azomethine (Schiff base) a structural unit of PAM, is common name of the molecules containing nitrogen–carbon double bonds (N=C). *N*-Benzylideneaniline is one of the representative molecules containing azomethine structures and the scaffold is easily synthesized by condensation reactions with benzaldehyde and aniline derivatives.[99] In addition, the *N*-benzylideneaniline skeleton is famous for a facile but useful rigid π-conjugated framework, and it is introduced into various functional materials.[17,99,100] Although the pristine azomethine scaffold hardly shows emission,[13] much more luminescent compounds have been produced by the boron complexation to

form robust structures compared to azo derivatives.[29–38,101] Similarly to azobenzene complexes, most of boron-fused azomethine luminophores have bidentate coordination. In this section, we explain luminescence properties of azomethine-based O,N,O-type tridentate coordination with o-salicylideneaminophenol derivatives and boron having tightly ring-fused structures. The obtained BAm complexes also showed "flexible and bendable" behaviors especially in the excited state as described in the previous sections. The BAm complexes exhibited more efficient luminescence properties than the BAz complexes in the shorter wavelength region. In addition, outstanding CIE properties,[45] thermosalient effect,[45] film-state emission in π-conjugated polymers[102], solid-state NIR emission in bisboron complexes,[103] controlling AIE and ACQ systems[104] were observed from the BAm materials. We introduce the unique characters of the BAm complexes from the recent studies.

2.1. Thermosalient effect and CIE

We prepared the BAm complex (**Et2N-BAm**) from o-salicylideneaminophenol modified by diethylamino group and boron (Figure 11a).[45] Recrystallization in THF under hexane atmosphere provided two polymorphic crystals, a yellow needle-like crystal (α) and an orange block crystal (β). **Et2N-BAm** showed an AIE behavior, that is, faint emission in a diluted solution state (Φ_{PL} = 0.001, 1.0×10^{-5} M in chloroform) and the slight emission enhancement was detected in amorphous state (Φ_{PL} = 0.003). Since the improvement was also observed under the dispersion condition in a polymer film (Φ_{PL} = 0.011), molecular motion in the excited state should affect the emission quenching, as seen in the BAz complexes. Theoretical calculation suggested that elongation of the bond length of N−C and bending of dihedral angle of C−N=C−C in

the excited state (1.42 Å and 114°, respectively) in comparison to those in the ground state (1.30 Å and 161°, respectively) (Figure 11b). The proposed bent motion of the BAm complex seemed to be more vigorous than that of BAz one because of the smaller bent angle. The "flexible and bendable" molecular motion should induce non-radiative deactivation of the excited energy.

Interestingly, **Et2N-BAm** showed distinct CIE properties because of larger emission enhancement in the crystalline states ($\Phi_{PL} = 0.39$ for crystal α and $\Phi_{PL} = 0.34$ for crystal β) than in the amorphous state. The value of k_r increased in the crystalline states ($k_r = 10^8$ s^{-1}) from that in amorphous state ($k_r = 10^5 \sim 10^6$ s^{-1}), meaning that crystallization enhances emission properties. Furthermore, we found crystal–crystal phase transition of **Et2N-BAm** by heating and cooling accompanied by alteration of emission color changes (Figure 11c). The α→β phase transition was induced by heating at around 80 °C, and the β→α phase transition was promoted by cooling at around −50 °C. Interestingly, the thermosalient effect which is thermally-induced hopping and fragmentation in molecular crystals was observed with the crystal–crystal phase transition. It is proposed that these mechanical behaviors should be associated with a very fast phase transition accompanied to anisotropic deformation (Figure 11d).[105] Thermosalient-active crystals are still rare and few examples were reported with emission color change.[106,107] Those extraordinary functionalities should be originated from the tightly-fused but "flexible and bendable" structure.

2.2. Highly efficient film-state emission

BAm is the monomeric structure of PAM which has relatively-high electron-accepting ability compared to PPV.[20] Therefore, we investigated the optical

properties of the D–A type π-conjugated polymers with fluorene (**BAmP-F**) and bithiophene (**BAmP-T**).[102] The BAm monomer (**BAmM**) had two alkyl chains to improve solubility and film-formability. The polymers in the absence of the boron-fused azomethine units (**AmP-F** and **AmP-T**) were also prepared as model compounds.

In UV–vis absorption spectra of **BAmP-F** and **BAmP-T** in chloroform (1.0×10^{-5} M), bathochromic shifts of the longest absorption bands were observed compared to that of the monomer **BAmM** (Figure 12). This result suggests that π-conjugation should be effectively elongated through the polymer main chain involving C=N bonds. **BAmP-T** showed larger bathochromic shift of absorption bands compared with the **BAmP-F**. It is because stronger electron-donating ability of bithiophene than that of fluorene can form robust electronic interaction with the BAm unit. Since the B–N coordination was able to enhance electron-accepting ability, the **BAmP-F** and **BAmP-T** performed further bathochromic shift of absorption compared to the corresponding ligand polymers (**AmP-F**, **AmP-T**).

In emission spectra, the ligand polymers, **AmP-F** and **AmP-T**, showed very weak emission (λ_{PL} = 461 nm, Φ_{PL} = 0.006 and λ_{PL} = 501 nm, Φ_{PL} = 0.002, respectively) as shown in the literature,[13] whereas the boron-fused polymers, **BAmP-F** and **BAmP-T**, exhibited intense emission in the solution state (λ_{PL} = 542 nm, Φ_{PL} = 0.24 and λ_{PL} = 627 nm, Φ_{PL} = 0.46, respectively). Surprisingly, the similar levels of emission efficiencies were detected in the film state (**BAmP-F**: Φ_{PL} = 0.29, λ_{em} = 553 nm; **BAmP-T**: Φ_{PL} = 0.30, λ_{em} = 637 nm). In general, wide π-surfaces of π-conjugated polymers are unfavorable for obtaining solid-state emission duet to ACQ caused by π–π interaction. The specific structure of BAm having the perpendicularly-protruded fluorine atom and two alkyl chains contributes to inhibiting non-specific interchain interactions in film.

The BAm unit has a potential to be a versatile "element-block" for realizing solid-state luminescent π-conjugated polymers. The LUMO energy levels of **BAmP-F** and **BAmP-T** were experimentally estimated to be −3.18 and −3.31 eV from CV, respectively. The absorption and emission wavelengths of **BAmP-F** and **BAmP-T** were dependent on the polarity of the solvents and Lippert–Mataga plots indicated that those bands were originated from the CT state. The BAm unit has a weaker electron-accepting ability than the BAz one (LUMO energy level: −3.8~4.0 eV), which is good agreement with the relationship of electron-accepting ability of PAM and PAZ. These data propose that the construction of π-conjugated polymers with the BAm unit is good strategy for obtaining visible luminescent materials both in solution and film states.

2.3. Bisboron complex with solid-state NIR emission

Emission annihilation in solution and AIE and CIE can be explained by the degree of molecular motions in the excited state. In this section, we evaluate precise effects of molecular rigidity and extension of π-conjugation on luminescent properties with the fully-fused bisboron complex (**bisBAm**).[103] **bisBAm** was synthesized as a mixture of diastereomers (*syn-* and *anti*-**bisBAm**) due to the two stereogenic boron centers (Figure 13a). The diastereomers were successfully separated by a reprecipitation method. By using solubility difference between soluble *syn*-**bisBAm** and insoluble *anti*-**bisBAm**, *anti*-**bisBAm** was selectively reprecipitated into diethyl ether from the chloroform solution of mixture of the diastereomers. In the crystal structure of *anti*-**bisBAm**, it was confirmed that the fully-fused structure with the relatively planar π-surface was covered by bulky three phenyl substituents around boron (Figure 13a).

The optical properties of *syn-* and *anti-***bisBAm** in comparison to those of the monoboron complex (**monoBAm**) were examined. Accordingly, absorption spectra of *syn-* and *anti-***bisBAm** in chloroform showed dramatical bathochromic shifts of the longest absorption bands (λ_{abs} = 599 and 595 nm, respectively) compared to that of **monoBAm** (λ_{abs} = 419 nm) (Figure 13b). This result is attributable to efficient extension of π-conjugation through the bisboron structure. Theoretical calculations supported that HOMO and LUMO of the **bisBAm** were delocalized over the entire molecules. Owing to the robust fully-fused structure of the bisboron complex, efficient emissions of *syn-* and *anti-***bisBAm** in solution were observed in the NIR region (λ_{PL} = 731 nm, Φ_{PL} = 0.035 and λ_{PL} = 729 nm, Φ_{PL} = 0.038, respectively) with large bathochromic shifts in the emission spectra from **monoBAm** (λ_{PL} = 522 nm, Φ_{PL} = 0.003) (Figure 13c). These exceptionally-large bathochromic shifts have never been reported in the previous literatures regarding π-conjugated multi-boron compounds.[36,108,109] Furthermore, it was revealed that **bisBAm** inherited solid-state emissive properties of the BAm unit. The solid-state NIR emissions of *syn-* and *anti-***bisBAm** were measured to be λ_{PL} = 757 nm (Φ_{PL} = 0.035) and λ_{PL} = 745 nm (Φ_{PL} = 0.052), respectively. It was proposed that three bulky phenyl groups around boron effectively prevented the chromophore unit from π–π stacking, followed by ACQ.

To evaluate the applicability of the **bisBAm** unit as a comonomer, the π-conjugated alternating copolymers composed of **bisBAm** and fluorene (**p-bisBAmF**) and bithiophene units (**p-bisBAmT**) were synthesized. From optical measurements, slight bathochromic shifts in absorption and emission spectra of **p-bisBAmF** and **p-bisBAmT** with enhancement of Φ_{PL} were observed in comparison to the monomer (**bisBAm**) (Figure 13a). Moreover, the polymers showed good film-state luminescence without

critical losses of Φ_{PL}. Those results indicate that **bisBAm** works as an emissive comonomer both in solution and film states. In should be noted that the differences between **p-bisBAmF** and **p-bisBAmT** were hardly detected. From the theoretical calculation, we assume that the delocalization of the HOMO might be mostly limited within the **bisBAm** scaffolds.

2.4. Design Strategy for AIE and CIE-active molecules

To obtain bright emission in solution, it is necessary to reinforce structural rigidity, for example, by the extension of π-conjugation through fully-fused bisboron complexes and polymer main chains. In the section, we proposed another strategy for preparing an emissive molecule in solution by employing the quinoline-based structures.[104] Furthermore, we demonstrate that these complexes are the typical example as the new design strategy for controlling ACQ and AIE molecules.

We synthesized two types of the quinoline-based boron complexes (Figure 14). **BPhQ** was synthesized from the tridentate quinoline ligand, and **BPhQm** had the methylene-inserted quinoline structure. From the comparison with single-crystal X-ray diffraction data, **BPhQ** had a relatively-distorted conformation with the dihedral angle between the quinoline and the adjacent phenyl ring as 154.7°. The distortion should be caused by the tightly-fused structure involving five and six membered rings around tetracoordinated boron. In contrast, **BPhQm** has a relatively planar structure (the dihedral angle = 168.8°) because of the loosely-fused two six-membered rings by the inserted methylene group.

From emission measurements, it was found that **BPhQm** showed emission in solution and ACQ in condensed state due to high planarity (Φ_{PL} = 0.21 in solution, Φ_{PL}

= 0.072 in aggregation, Φ_{PL} = 0.051 in crystal). On the other hand, **BPhQ** exhibited typical AIE and CIE properties because of the distorted structure (Φ_{PL} = 0.008 in solution, Φ_{PL} = 0.014 in aggregation, Φ_{PL} = 0.017 in crystal). The emission quenching in solution suggested that large degree of molecular motion should occur in **BPhQ** after photo-excitation because of intrinsic skeletal distortion. From the comparison of the crystal packing structures, the different optical behaviors were probably caused by the planarity of **BPhQ** and **BPhQm**. In **BPhQ**, two types of the distances between intermolecular π–π interactions (3.596 and 4.148 Å) were detected (Figure 14). Therefore, intermolecular π–π interactions through multi molecules were inhibited owing to steric hindrance imposed by the distorted π-conjugated system. In contrast, the high planarity of **BPhQm** induced densely packed molecular columns which form face-to-face π–π interactions between both surfaces with distances of 3.723 and 3.807 Å (Figure 14). Considering the results of emission measurements, it is proposed that the inhibition of consecutive π–π interactions with the distorted structure of **BPhQ** is effective for avoiding ACQ. On the other hand, the tight intermolecular π–π interactions with the planar structure of **BPhQm** resulted in critical ACQ. We clearly show that AIE and CIE or ACQ can be controlled with or without structural distortion caused by the insertion of the methylene unit. This should offer the new design strategy based on the introduction of distortion with boron complexation for realizing AIE and CIE properties.

3. Summary and Outlook

We introduced unique and versatile optical properties originating from "flexible and bendable" boron-fused azomethine and azobenzene complexes (BAm and BAz)

with the O,N,O-type tridentate ligands, respectively. It was demonstrated that bending and movable π-conjugated structures composed of perpendicularly-protruded substituents at the boron atom were a key unit for expressing AIE and CIE properties. Additionally, environment-sensitive behaviors, such as thermosalient effects with luminochromic properties during crystal–crystal transition were also observed. Furthermore, π-conjugated polymers involving these units can exhibit intense emission both in solution and film states. By the combination with electron-accepting ability of the complexes and electron-donating comonomers, the D–A type polymers with highly-efficient emissions in the NIR region can be obtained. Narrow energy gaps between FMOs were also realized by constructing the PPV-analogue structure. From our results described here, it can be said that the azomethine and azobenzene units could be a promising "element-block" for developing advanced functional materials according to precise designs.

Acknowledgement
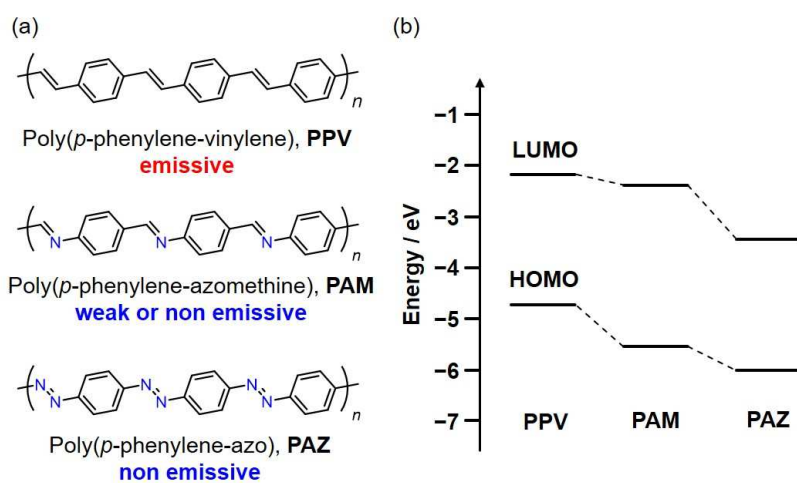
Figure 1. Structures and energy revels of HOMO and LUMO of π-conjugated polymers, PPV, PAM and PAZ. Reprinted with permission from ref 20. Copyright 2005 Elsevier.
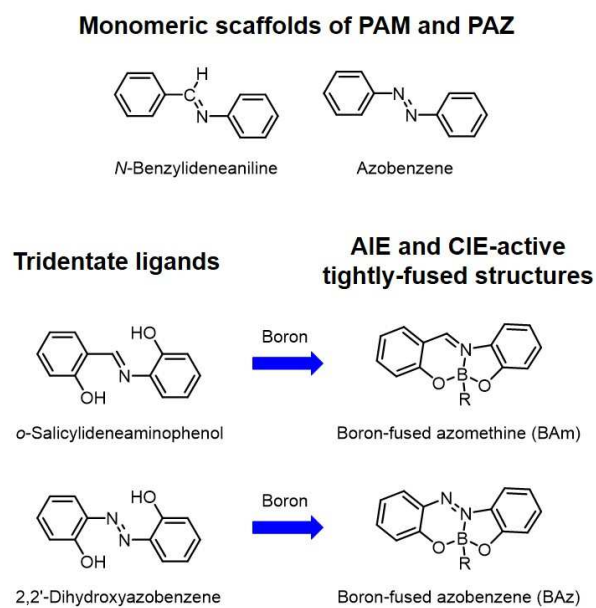
Figure 2. Structures of the azomethine and azobenzene derivatives and boron complexes with O,N,O-type tridentate ligands. Reprinted with permission from ref 50. Copyright 2019 The Chemical Society of Japan.

"Flexible and Bendable"

planar   bent

ground state   excited state
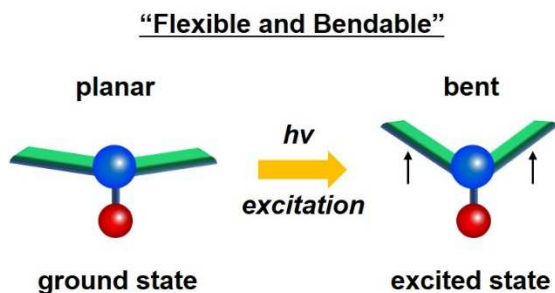
Figure 3. Excitation-driven molecular motion in BAm and BAz. Reprinted with permission from ref 50. Copyright 2019 The Chemical Society of Japan.
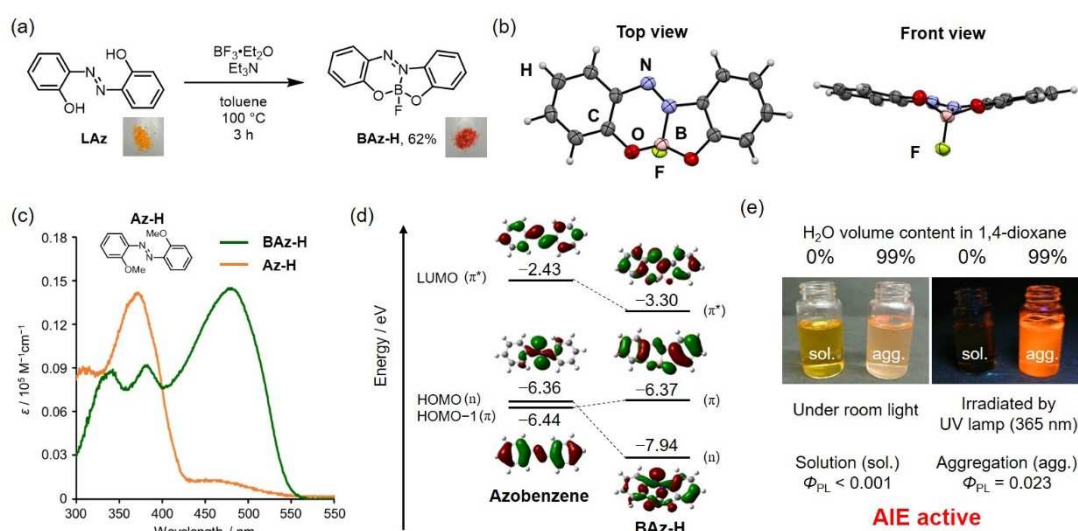
Figure 4. The functionalities of **BAz-H**. (a) Synthesis of **BAz-H** from **LAz** and their colors. (b) ORTEP drawings of **BAz-H** from results of single crystal X-ray structural analysis. (c) UV–vis absorption spectra of **BAz-H** and **Az-H** in toluene (1.0×10^{-5} M). (d) Energy diagram, selected MOs of azobenzene and **BAz-H** with DFT calculation at B3LYP/6-311G(d,p) level (isovalue = 0.03). (e) AIE properties of **BAz-H**. Reprinted with permission from ref 46. Copyright 2018 WILEY-VCH Verlag GmbH & Co. KGaA, Weinheim.
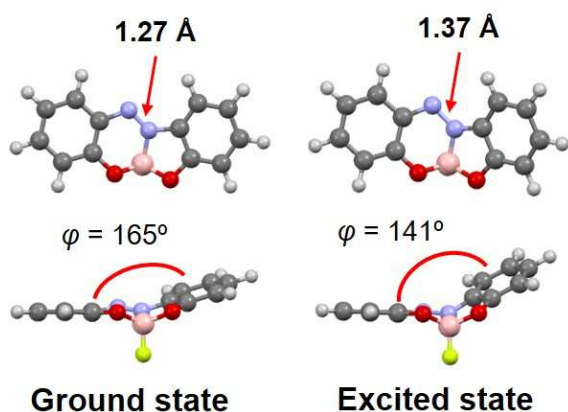
Figure 5. Optimized structures in the ground and excited states of **BAz-H** with DFT and TD-DFT calculations at the B3LYP/6-311G(d,p) and TD-B3LYP/6-311+G(d,p) levels, respectively. Reprinted with permission from ref 46. Copyright 2018 WILEY-VCH Verlag GmbH & Co. KGaA, Weinheim.
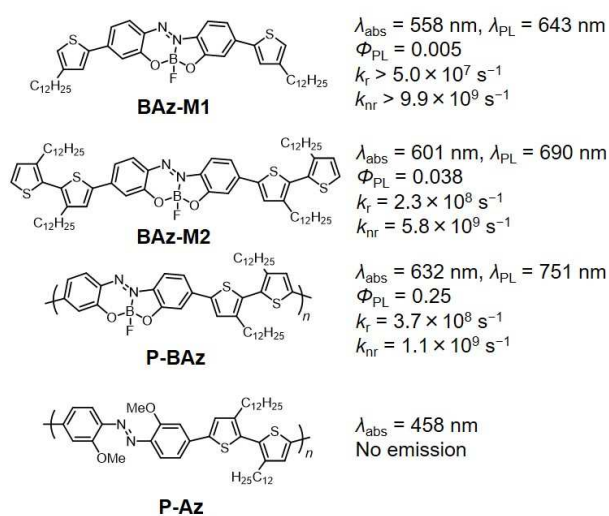
Figure 6. Optical properties of oligomers and polymers in toluene (1.0×10^{-5} M per repeating unit).
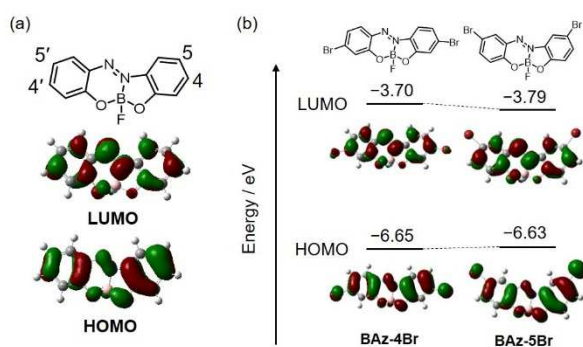
Figure 7. (a) Substituent positions of **BAz-H**. (b) Energy diagram and MOs of **BAz-4Br** and **BAz-5Br** with DFT calculation at B3LYP/6-311+G(2d,p) level (isovalue = 0.03). Reprinted with permission from ref 86. Copyright 2019 WILEY-VCH Verlag GmbH & Co. KGaA, Weinheim.

(a)

P-BAz-5BT
LUMO: −4.03 eV
λ_{abs} = 600 nm, λ_{PL} = 779 nm
Φ_{PL} < 0.01

P-BAz-4BT
LUMO: −3.98 eV
λ_{abs} = 632 nm, λ_{PL} = 751 nm
Φ_{PL} = 0.25

(b)

M-BAz-5BT-Me   **M-BAz-4BT-Me**

LUMO   LUMO

HOMO   HOMO
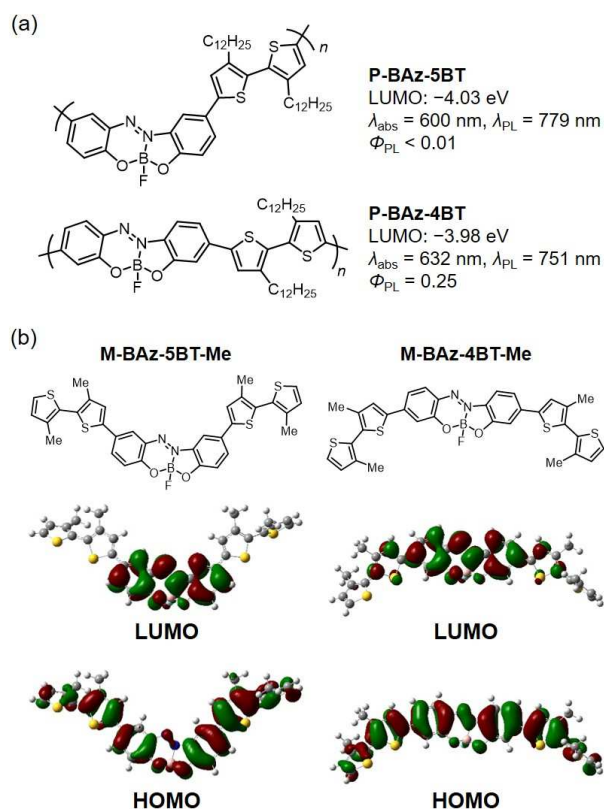
Figure 8. (a) Energy levels of LUMO and optical properties of polymers in diluted toluene. (b) MOs of model compounds with DFT calculation at B3LYP/6-311G(d,p) level (isovalue = 0.02). Reprinted with permission from ref 86. Copyright 2019 WILEY-VCH Verlag GmbH & Co. KGaA, Weinheim.
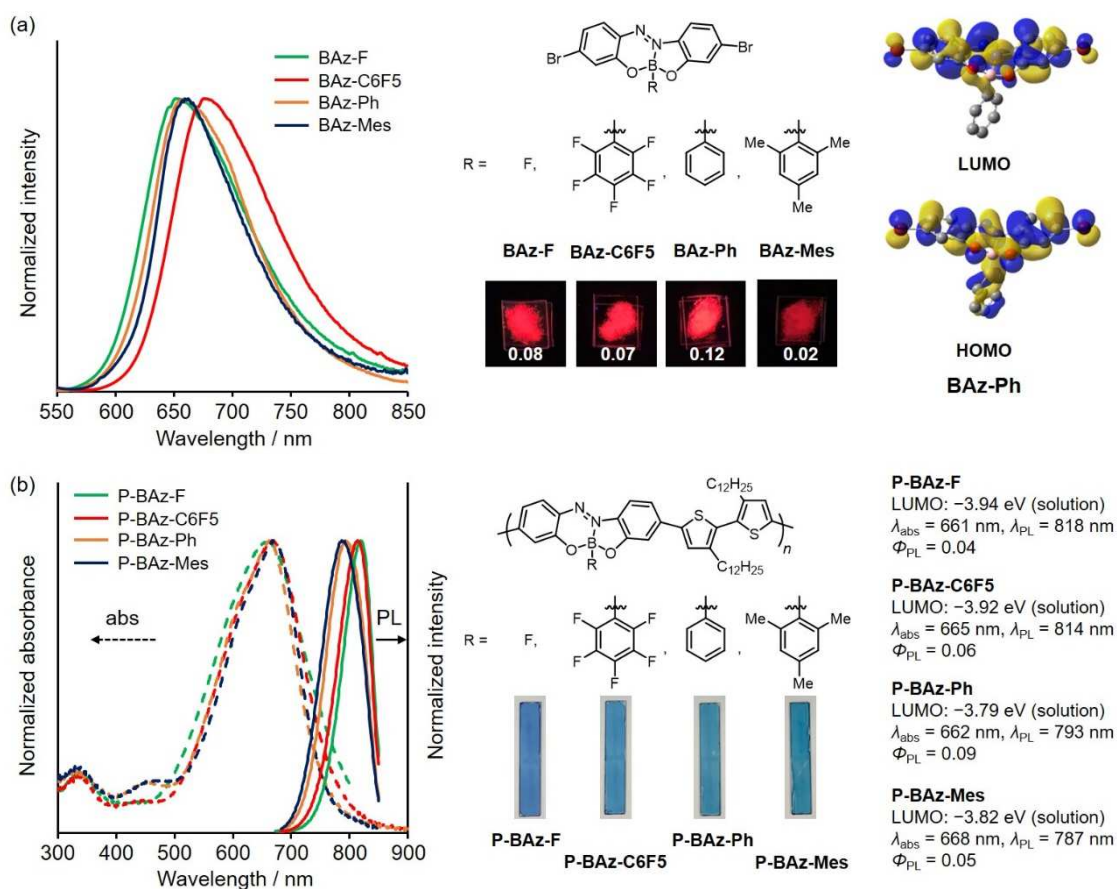
Figure 9. (a) Emission spectra in crystals, chemical structures, photos of luminescence properties with Φ_{PL}s and MOs (DFT calculation: B3LYP/6-311G(d,p) level (isovalue = 0.02)) of the BAz complexes. (b) UV–vis–NIR absorption and emission spectra in films, chemical structures, photos of films with optical properties of the BAz polymers. Reprinted with permission from ref 87. Copyright 2020 WILEY-VCH Verlag GmbH & Co. KGaA, Weinheim.
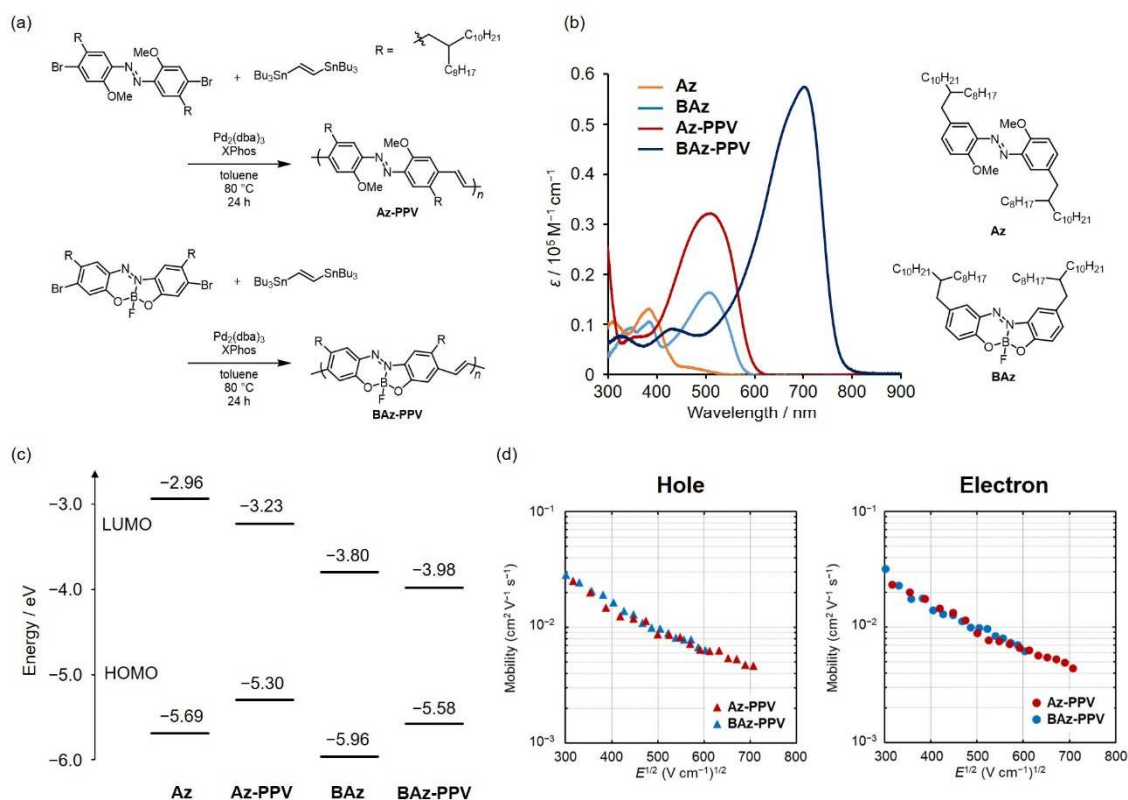
Figure 10. (a) Syntheses of **Az-PPV** and **BAz-PPV**. (b) UV–vis–NIR absorption spectra in toluene (1.0×10^{-5} M for monomers, 1.0×10^{-5} M per repeating unit for polymers) and (c) energy diagram of MOs of BAz complexes. (d) Electron and hole mobilities of **Az-PPV** and **BAz-PPV** measured by a time-of flight technique with the device composed of ITO (50 nm)/**Az-PPV** (8 μm) or **BAz-PPV** (11 μm)/Al ($\approx$ 50 nm). Reprinted with permission from ref 65. Copyright 2020 American Chemical Society.
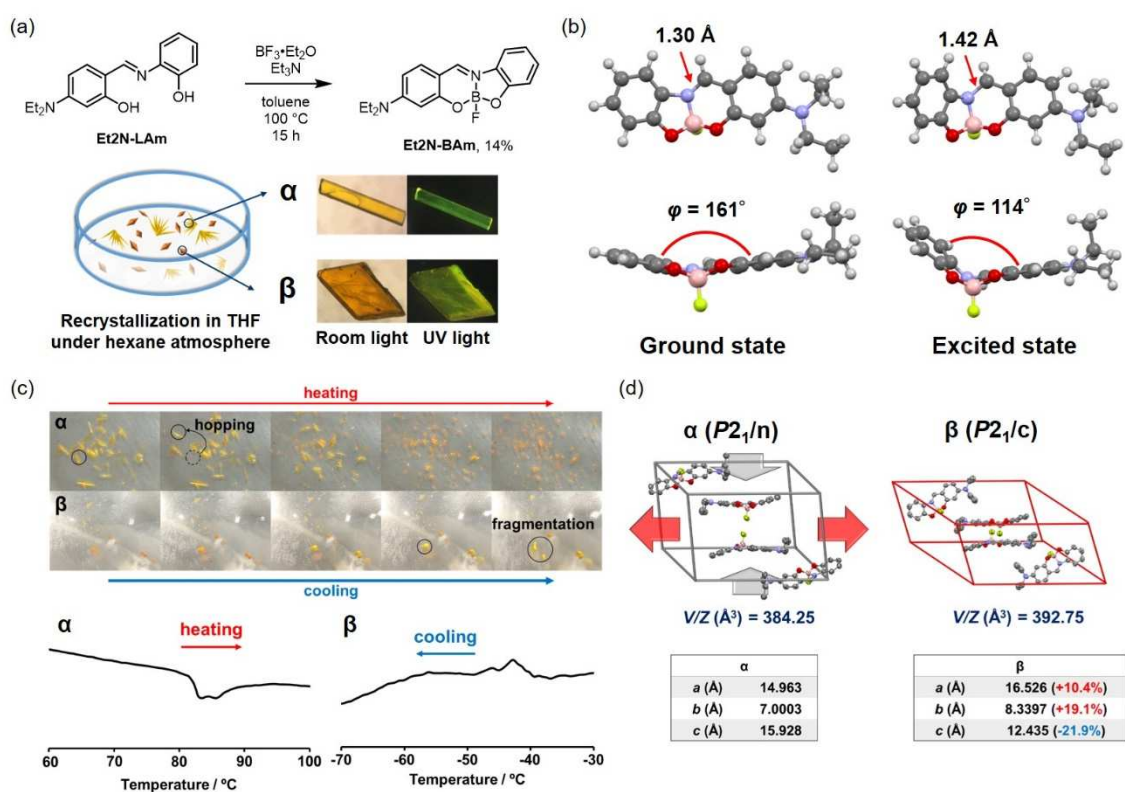
Figure 11. (a) Synthesis of **Et2N-BAm** and separation of the polymorph. (b) Optimized structures in the ground and excited states of **Et2N-BAm** with DFT and TD-DFT calculations at the B3LYP/6-311G(d,p) and TD-B3LYP/6-311+G(d,p) levels, respectively. (c) Snapshots of thermosalient behaviors and DSC curves of crystal α and β. (d) Anisotropic deformation of unit cells of α and β during α→β crystal–crystal transition. Reprinted with permission from ref 45. Copyright 2017 WILEY-VCH Verlag GmbH & Co. KGaA, Weinheim.

AmM
LUMO: −2.73 eV (solution)
$\lambda_{abs,solution}$ = 339 nm, no emission

AmP-F Φ_{PL} = 0.006
LUMO: −2.67 eV (solution)
$\lambda_{abs,solution}$ = 387 nm, $\lambda_{PL,solution}$ = 461 nm

AmP-T Φ_{PL} = 0.002
LUMO: −2.73 eV (solution)
$\lambda_{abs,solution}$ = 409 nm, $\lambda_{PL,solution}$ = 501 nm

BAmM
LUMO: −3.27 eV (solution)
$\lambda_{abs,solution}$ = 385 nm, $\lambda_{PL,solution}$ = 473 nm
Φ_{PL} = 0.016

BAmP-F Φ_{PL} = 0.29 0.29
LUMO: −3.18 eV (solution)
$\lambda_{abs,solution}$ = 439 nm, $\lambda_{PL,solution}$ = 542 nm
$\lambda_{abs,film}$ = 449 nm, $\lambda_{PL,film}$ = 553 nm

BAmP-T Φ_{PL} = 0.45 0.30
LUMO: −3.31 eV (solution)
$\lambda_{abs,solution}$ = 483 nm, $\lambda_{PL,solution}$ = 627 nm
$\lambda_{abs,film}$ = 478 nm, $\lambda_{PL,film}$ = 637 nm

Figure 12. (a) Structures and optical properties of BAm monomers and polymers with photos in solution and film states irradiated by UV lamp (365 nm). Reprinted with permission from ref 102. Copyright 2020 American Chemical Society.
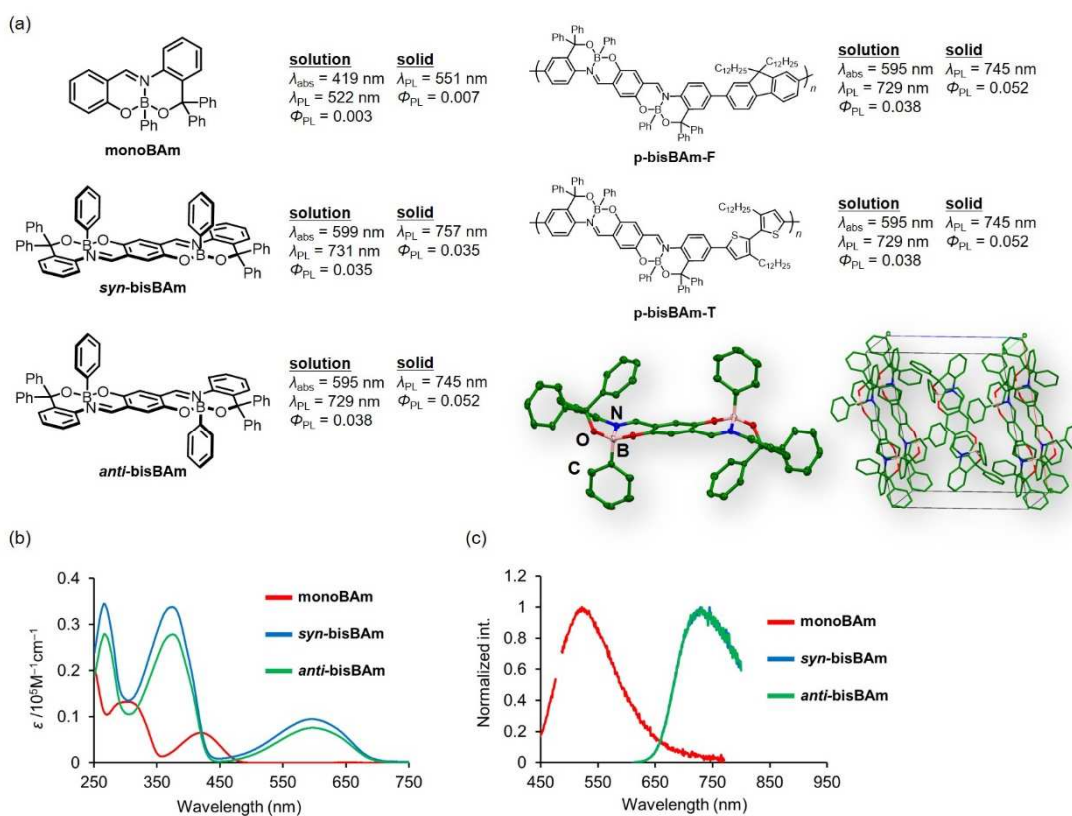
Figure 13. (a) Structures and optical properties of **monoBAm**, **bisBAm** and polymers, and an ORTEP drawing and a crystal packing of **_anti_-bisBAm** where hydrogen atoms are omitted for clarity. (b) UV–vis–NIR absorption and (c) emission spectra of **monoBAm** and **bisBAm** in chloroform (1.0×10^{-5} M). Reprinted with permission from ref 103. Copyright 2020 The Royal Society of Chemistry.
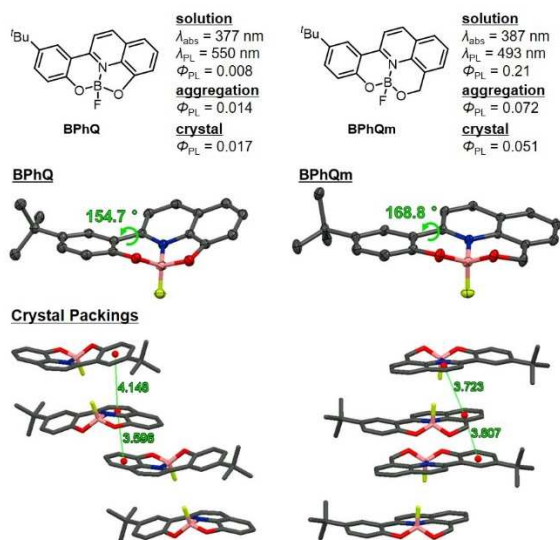
Figure 14. Structures, optical properties, ORTEP drawings and crystal packing structures of **BPhQ** and **BPhQm**. Hydrogen atoms are omitted for clarity. Reprinted with permission from ref 104. Copyright 2020 MDPI (Basel, Switzerland).

References

[1]   S. Nakamura, *Science* **1998**, *281*, 956–961.

[2]   M. R. Krames, O. B. Shchekin, R. Mueller-Mach, G. O. Mueller, L. Zhou, G. Harbers, M. G. Craford, *J. Disp. Technol.* **2007**, *3*, 160–175.

[3]   J. Song, H. Lee, E. G. Jeong, K. C. Choi, S. Yoo, *Adv. Mater.* **2020**, *32*, 1907539.

[4]   H. Sasabe, J. Kido, J. *Mater. Chem. C* **2013**, *1*, 1699–1707.

[5]   J. Shi, S. Liu, L. Zhang, B. Yang, L. Shu, Y. Yang, M. Ren, Y. Wang, J. Chen, W. Chen, Y. Chai, X. Tao, *Adv. Mater.* **2020**, *32*, 1901958.

[6]   T. Yamamoto, *Macromol. Rapid Commun.* **2002**, *23*, 583–606.

[7]   X. Guo, M. Baumgarten, K. Müllen, *Prog. Polym. Sci.* **2013**, *38*, 1832–1908.

[8]   A. Facchetti, *Chem. Mater.* **2011**, *23*, 733–758.

[9]   M. S. AlSalhi, J. Alam, L. A. Dass, M. Raja, *Int. J. Mol. Sci.* **2011**, *12*, 2036–2054.

[10]   A. J. Blayney, I. F. Perepichka, F. Wudl, D. F. Perepichka, *Isr. J. Chem.* **2014**, *54*, 674–688.

[11]   N. C. Greenham, S. C. Moratti, D. D. C. Bradley, R. H. Friend, A. B. Holmes, *Nature* **1993**, *365*, 628–630.

[12]   M. Kuik, G.-J. A. H. Wetzelaer, H. T. Nicolai, N. I. Craciun, D. M. De Leeuw, P. W. M. Blom, *Adv. Mater.* **2014**, *26*, 512–531.

[13]   C.-P. Chang, C.-C. Wang, C.-Y. Chao, M.-S. Lin, *J. Polym. Res.* **2005**, *12*, 1–7.

[14]   A. Izumi, R. Nomura, T. Masuda, *Macromolecules* **2001**, *34*, 4342–4347.

[15]   N. Kawatsuki, T. Washio, J. Kozuki, M. Kondo, T. Sasaki, H. Ono, *Polymer* **2015**, *56*, 318–326.

[16]   P. Weis, S. Wu, *Macromol. Rapid Commun.* **2017**, *39*, 1700220.

[17]   I. Janica, V. Patroniak, P. Samorì, A. Ciesielski, *Chem. Asian J.* **2018**, *13*, 465–481.

[18]   A. Chevalier, P.-Y. Renard, A. Romieu, *Chem. Asian J.* **2017**, *12*, 2008–2028.

[19]   H. Yu, *J. Mater. Chem. C* **2014**, *2*, 3047–3054.

[20]   C.-L. Liu, F.-C. Tsai, C.-C. Chang, K.-H. Hsieh, J.-L. Lin, W.-C. Chen, *Polymer* **2005**, *46*, 4950–4957.

[21]   Y. Chujo, K. Tanaka, *Bull. Chem. Soc. Jpn.* **2015**, *88*, 633–643.

[22]   M. Gon, K. Tanaka, Y. Chujo, *Polym. J.* **2018**, *50*, 109–126.

[23]   K. Tanaka, Y. Chujo, *Polym. J.* **2020**, *52*, 555–566.

[24]   K. Tanaka, Y. Chujo, *Macromol. Rapid Commun.* **2012**, 33, 1235–1255.

[25]   A. Loudet, K. Burgess, *Chem. Rev.* **2007**, 107, 4891–4932.

[26]   J. Yoshino, N. Kano, T. Kawashima, *Chem. Commun.* **2007**, 559–561.

[27]   J. Yoshino, A. Furuta, T. Kambe, H. Itoi, N. Kano, T. Kawashima, Y. Ito, M. Asashima, *Chem. Eur. J.* **2010**, *16*, 5026–5035.

[28]   N. Kano, A. Furuta, T. Kambe, J. Yoshino, Y. Shibata, T. Kawashima, N. Mizorogi, S. Nagase, *Eur. J. Inorg. Chem.* **2012**, 1584–1587.

[29]   J. Yoshino, N. Kano, T. Kawashima, *Dalton Trans.* **2013**, *42*, 15826–15834.

[30]   J. Yoshino, N. Kano, T. Kawashima, *J. Org. Chem.* **2009**, *74*, 7496–7503.

[31]   J. Yoshino, N. Kano, T. Kawashima, T. *Bull. Chem. Soc. Jpn*. **2010**, *83*, 1185–1187.

[32]   D. Frath, S. Azizi, G. Ulrich, P. Retailleau, R. Ziessel, *Org. Lett.* **2011**, *13*, 3414–3417.

[33]   D. Frath, S. Azizi, G. Ulrich, R. Ziessel, *Org. Lett.* **2012**, *14*, 4774–4777.

[34] D. Frath, P. Didier, Y. Mély, J. Massue, G. Ulrich, *ChemPhotoChem* **2017**, *1*, 109–112.

[35] J. Dobkowski, P. Wnuk, J. Buczyńska, M. Pszona, G. Orzanowska, D. Frath, G. Ulrich, J. Massue, S. Mosquera-Vázquez, E. Vauthey, C. Radzewicz, R. Ziessel, J. Waluk, *Chem. Eur. J.* **2015**, *21*, 1312–1327.

[36] M. Urban, K. Durka, P. Jankowski, J. Serwatowski, S. Luliński, *J. Org. Chem.* **2017**, *82*, 8234–8241.

[37] G. Wesela-Bauman, M. Urban, S. Luliński, J. Serwatowski, K. Woźniak, *Org. Biomol. Chem.* **2015**, *13*, 3268–3279.

[38] P. Zhang, W. Liu, G. Niu, H. Xiao, M. Wang, J. Ge, J. Wu, H. Zhang, Y. Li, P. Wang, *J. Org. Chem.* **2017**, *82*, 3456–3462.

[39] F. Umland, E. Hohaus, K. Brodte, *Chem. Ber.* **1973**, *106*, 2427–2437.

[40] E. Hohaus, W. Riepe, K. Wessendorf, *Z. Naturforsch. B* **1980**, 35B, 316–318.

[41] E. Hohaus, W. Wessendorf, *Z. Naturforsch. B* **1980**, 35B, 319–325.

[42] M. Rodríguez, M. E. Ochoa, R. Santillan, N. Farfán, V. Barba, *J. Organomet. Chem.* **2005**, *690*, 2975–2988.

[43] H. López-Ruiz, I. Mera-Moreno, S. Rojas-Lima, R. Santillán, N. Farfán, *Tetrahedron Lett.* **2008**, *49*, 1674–1677.

[44] H. Reyes, B. M. Muñoz, N. Farfán, R. Santillan, S. Rojas-Lima, P. G. Lacroix, K. Nakatani, *J. Mater. Chem.* **2002**, *12*, 2898–2903.

[45] S. Ohtani, M. Gon, K. Tanaka, Y. Chujo, *Chem. Eur. J.* **2017**, *23*, 11827–11833.

[46] M. Gon, K. Tanaka, Y. Chujo, *Angew. Chem. Int. Ed.* **2018**, *57*, 6546–6551; *Angew. Chem.* **2018**, *130*, 6656–6661.

[47] J. Mei, N. L. C. Leung, R. T. K. Kwok, J. W. Y. Lam, B. Z. Tang, *Chem. Rev.* **2015**, *115*, 11718–11940.

[48] J. Luo, Z. Xie, J. W. Y. Lam, L. Cheng, H. Chen, C. Qiu, H. S. Kwok, X. Zhan, Y. Liu, D. Zhu, B. Z. Tang, *Chem. Commun.* **2001**, 1740–1741.

[49] S. A. Jenekhe and J. A. Osaheni, *Science* **1994**, 265, 765–768.

[50] M. Gon, K. Tanaka, Y. Chujo, *Bull. Chem. Soc. Jpn.* **2019**, *92*, 7–18.

[51] Y. Dong, J. W. Y. Lam, A. Qin, Z. Li, J. Sun, H. H.-Y. Sung, I. D. Williams, B. Z. Tang, *Chem. Commun.* **2007**, 40–42.

[52] R. Yoshii, A. Nagai, K. Tanaka, Y. Chujo, *Chem. Eur. J.* **2013**, *19*, 4506–4512.

[53] R. Yoshii, K. Tanaka, Y. Chujo, *Macromolecules* **2014**, *47*, 2268–2278.

[54] R. Yoshii, K. Suenaga, K. Tanaka, Y. Chujo, *Chem. Eur. J.* **2015**, *21*, 7231–7237.

[55] K. Suenaga, R. Yoshii, K. Tanaka, Y. Chujo, *Macromol. Chem. Phys.* **2016**, *217*, 414–421.

[56] K. Suenaga, K. Uemura, K. Tanaka, Y. Chujo, *Polym. Chem.* **2020**, *11*, 1127–1133.

[57] R. Yoshii, A. Hirose, K. Tanaka, Y. Chujo, *Chem. Eur. J.* **2014**, *20*, 8320–8324.

[58] R. Yoshii, A. Hirose, K. Tanaka, Y. Chujo, *J. Am. Chem. Soc.* **2014**, *136*, 18131–18139.

[59] S. Ito, A. Hirose, M. Yamaguchi, K. Tanaka, Y. Chujo, *J. Mater. Chem. C* **2016**, *3*, 5564–5571.

[60] M. Yamaguchi, S. Ito, A. Hirose, K. Tanaka, Y. Chujo, *J. Mater. Chem. C* **2016**, *3*, 5314–5319.

[61] M. Yamaguchi, S. Ito, A. Hirose, K. Tanaka, Y. Chujo, *Mater. Chem. Front.* **2017**, 1, 1573–1579.

[62]   M. Yamaguchi, S. Ito, A. Hirose, K. Tanaka, Y. Chujo, *Polym. Chem.* **2018**, *9*, 1942–1946.

[63]   A. Wakamiya, T. Taniguchi, S. Yamaguchi, *Angew. Chem. Int. Ed.* **2006**, *45*, 3170–3173; *Angew. Chem.* **2006**, *118*, 3242–3245.

[64]   M. M. Alam, S. A. Jenekhe, *Chem. Mater.* **2004**, *16*, 4647–4656.

[65]   J. Wakabayashi, M. Gon, K. Tanaka, Y. Chujo, *Macromolecules* **2020**, *53*, 4524–4532.

[66]   G. Padmanaban, S. Ramakrishnan, *J. Am. Chem. Soc.* **2000**, *122*, 2244–2251.

[67]   H. Meier, U. Stalmach, H. Kolshorn, *Acta Polym.* **1997**, *48*, 379-384.

[68]   M. Kosugi, K. Sasazawa, Y. Shimizu, T. Migita, *Chem. Lett.* **1977**, *6*, 301–302.

[69]   D. Milstein, J. K. Stille, *J. Am. Chem. Soc.* **1978**, *100*, 3636–3638.

[70]   E. Merino, *Chem. Soc. Rev.* **2011**, *40*, 3835–3853.

[71]   M. Zhu, H. Zhou, *Org. Biomol. Chem.* **2018**, *16*, 8434–8445.

[72]   R. C. Advincula, E. Fells, M. Park, *Chem. Mater.* **2001**, *13*, 2870–2878.

[73]   H. Akiyama, A. Tanaka, H. Hiramatsu, J. Nagasawa, N. Tamaoki, *J. Mater. Chem.* **2009**, *19*, 5956–5963.

[74]   Cembran, A.; Bernardi, F.; Garavelli, M.; Gagliardi, L.; Orlandi, G. *J. Am. Chem. Soc.* **2004**, *126*, 3234–3243.

[75]   T. Fujino, S. Y. Arzhantsev, T. Tahara, *J. Phys. Chem. A* **2001**, *105*, 8123–8129.

[76]   Bandara, H. M. D.; Burdette, S. C. *Chem. Soc. Rev.* **2012**, *41*, 1809–1825.

[77]   Rau, H. *Angew. Chem. Int. Ed. Engl.* **1973**, *12*, 224–235; *Angew. Chem.* **1973**, *85*, 248–258.

[78]   M. Ghedini, D. Pucci, G. Calogero, F. Barigelletti, *Chem. Phys. Lett.* **1997**, *267*, 341–344.

[79] G. Gabor, Y. Frei, D. Gegiou, M. Kaganowitch, E. Fischer, *Isr. J. Chem.* **1967**, *5*, 193–211.

[80] H. M. D. Bandara, T. R. Friss, M. M. Enriquez, W. Isley, C. Incarvito, H. A. Frank, J. Gascon, S. C. Burdette, *J. Org. Chem.* **2010**, *75*, 4817–4827.

[81] M. Han, S. J. Cho, Y. Norikane, M. Shimizu, A. Kimura, T. Tamagawa, T. Seki, *Chem. Commun.* **2014**, *50*, 15815–15818.

[82] A.-Y. Jee, Y. Lee, M. Lee, M. H. Kim, *J. Chem. Phys.* **2012**, *136*, 121104.

[83] M. Yamauchi, K. Yokoyama, N. Aratani, H. Yamada, S. Masuo, *Angew. Chem. Int. Ed.* **2019**, *58*, 14173–14178; *Angew. Chem.* **2019**, *131*,14311–14316.

[84] Q. Zhu, S. Wang, P. Chen, *Org. Lett.* **2019**, *21*, 4025–4029.

[85] F. Bu, R. Duan, Y. Xie, Y. Yi, Q. Peng, R. Hu, A. Qin, Z. Zhao, B. Z. Tang, *Angew. Chem. Int. Ed.* **2015**, *54*, 14492–14497; *Angew. Chem.* **2015**, *127*, 14700–14705.

[86] M. Gon, J. Wakabayashi, K. Tanaka, Y. Chujo, *Chem. Asian J.* **2019**, *14*, 1837–1843.

[87] M. Gon, J. Wakabayashi, M. Nakamura, K. Tanaka, Y. Chujo, *Macromol. Rapid Commun.* **2020**, 2000566. DOI:10.1002/marc.202000566.

[88] A. Zampetti, A. Minotto, F. Cacialli, *Adv. Funct. Mater.* **2019**, *29*, 1807623.

[89] H. Xiang, J. Cheng, X. Ma, X. Zhou, J. J. Chruma, *Chem. Soc. Rev.* **2013**, *42*, 6128–6185.

[90] L. Yuan, W. Lin, K. Zheng, L. He, W. Huang, *Chem. Soc. Rev.* **2013**, *42*, 622–661.

[91] R. Mauer, M. Kastler, F. Laquai, *Adv. Funct. Mater.* **2010**, *20*, 2085–2092.

[92] E. Lebedev, T. Dittrich, V. Petrova-Koch, S. Karg, W. Brütting, *Appl. Phys. Lett.* **1997**, *71*, 2686–2688.

[93] S. H. Lee, T. Yasuda, T. Tsutsui, *J. Appl. Phys.* **2004**, *95*, 3825–3827.

[94] Q. Shi, Y. Hou, H. Jin, Y. Li, *J. Appl. Phys.* **2007**, *102*, 073108.

[95] S. S. Pandey, W. Takashima, S. Nagamatsu, T. Endo, M. Rikukawa, K. Kaneto, *Jpn. J. Appl. Phys.* **2000**, *39*, L94–L97.

[96] S. S. Pandey, W. Takashima, T. Endo, M. Rikukawa, K. Kaneto, *Synth. Met.* **2001**, *121*, 1561–1562.

[97] A. Babel, S. A. Jenekhe, *Macromolecules* **2003**, *36*, 7759–7764.

[98] K. Ueda, K. Tanaka, Y. Chujo, *Polymers* **2018**, *11*, 44.

[99] J. L. Segura, M. J. Mancheño, F. Zamora, *Chem. Soc. Rev.* **2016**, 45, 5635–5671.

[100] J. Zhang, L. Xu, W.-Y. Wong, *Coord. Chem. Rev.* **2018**, *355*, 180–198.

[101] C. C. Vidyasagar, B. M. Muñoz Flores, V. M. Jiménez-Pérez, P. M. Gurubasavaraj, *Mater. Today Chem.* **2019**, *11*, 133–155.

[102] S. Ohtani, M. Gon, K. Tanaka, Y. Chujo, *Macromolecules* **2019**, *52*, 3387–3393.

[103] S. Ohtani, M. Nakamura, M. Gon, K. Tanaka, Y. Chujo, *Chem. Commun.* **2020**, *56*, 6575–6578.

[104] S. Ohtani, M. Gon, K. Tanaka, Y. Chujo, *Crystals* **2020**, *10*, 615.

[105] P. Commins, I. T. Desta, D. P. Karothu, M. K. Panda, P. Naumov, *Chem. Commun.* **2016**, *52*, 13941–13954.

[106] T. Takeda, T. Akutagawa, *Chem. Eur. J.* **2016**, *22*, 7763–7770.

[107] S. C. Sahoo, M. K. Panda, N. K. Nath, P. Naumov, *J. Am. Chem. Soc.* **2013**, *135*, 12241–12251.

[108] Z. Zhang, H. Bi, Y. Zhang, D. Yao, H. Gao, Y. Fan, H. Zhang, Y. Wang, Y. Wang, Z. Chen, D. Ma, *Inorg. Chem.* **2009**, *48*, 7230–7236.

[109] D. Li, K. Wang, S. Huang, S. Qu, X. Liu, Q. Zhu, H. Zhang and Y. Wang, *J. Mater. Chem.* **2011**, *21*, 15298–15304.